Proc. 31st Int. Workshop on Vertex Detectors (VERTEX2022)
JPS Conf. Proc. **42**, 011031 (2024)
https://doi.org/10.7566/JPSCP.42.011031

TCAD simulations of innovative Low-Gain Avalanche Diodes for particle detector design and optimization

Francesco MOSCATELLI [1,2*], Tommaso CROCI[2], Valentina SOLA[3,4], Daniele PASSERI[5] and Arianna MOROZZI[2]

[1] *CNR-IOM of Perugia, via A. Pascoli 23c, 06123 Perugia, Italy.*
[2]*INFN section of Perugia, via A. Pascoli 23c, 06123 Perugia, Italy.*
[3]*University of Torino, via P. Giuria 1, 10125, Torino, Italy.*
[4]*INFN of Torino, via P. Giuria 1, 10125, Torino, Italy.*
[5] *University of Perugia, Department of Engineering, via G. Duranti 93, 06125 Perugia, Italy.*

**E-mail: moscatelli@iom.cnr.it*

(Received December 16, 2022)

In this work the results of Technology-CAD (TCAD) device-level simulations of non-irradiated and irradiated Low-Gain Avalanche Diode (LGAD) detectors will be presented. Since LGADs are becoming one of the most promising devices for high performance particle detector in harsh radiation environments, it is of the utmost importance to have a predictive insight into their electrical behavior and charge collection properties up to the highest particle fluences reachable, for example, in the future High Energy Physics (HEP) experiments. To this purpose, state-of-the-art Synopsys Sentaurus TCAD tools have been adopted and equipped with a well-validated radiation damage numerical model, called the "New University of Perugia" model. The model has been coupled with an analytical description of the peculiar mechanism of acceptor removal in the multiplication layer affecting irradiated LGAD devices. Thanks to this, it has been possible to reproduce experimental data with high accuracy, demonstrating the reliability of the implemented simulation framework. Moreover, the good agreement obtained between simulation results and experimental data has allowed us to apply the newly developed model for the optimization of two innovative paradigms for the design of LGAD sensors for 4D tracking, namely *i)* compensated LGAD and *ii)* DC-Coupled Resistive Silicon Detectors (DC-RSD) LGADs. The first option refers to a new design of the gain layer implant that, by combining p^+ and n^+ dopants, has the potential to maintain a constant active doping density after very high irradiation. The second option is an evolution of RSD design that employs DC read-out with low resistivity strips between collecting pads. The obtained results will provide all the necessary information for the design of the first production batches of "compensated LGAD" and DC-RSD at Fondazione Bruno Kessler (FBK) foundry in Trento, Italy.

KEYWORDS: LGAD; radiation damage effects; radiation hardness; TCAD numerical simulations.

1. Introduction

The next generation of hadron colliders for particle physics will require tracking

detectors able to efficiently record charged particles in harsh radiation environments, where expected fluences exceed 10^{17} (1MeV) n_{eq}/cm^2. Presently available silicon sensors can operate efficiently up to fluences of the order of 10^{16} n_{eq}/cm^2. Therefore, one of the most important goals of present R&Ds on silicon sensors is to increase their radiation tolerance by more than an order of magnitude. For this reason, several R&D activities are ongoing in different laboratories worldwide to develop the next generation of particle detectors, which will be able to fulfill the stringent technical specifications deriving from this new operating scenario [1].

Low-Gain Avalanche Diodes (LGADs) are becoming one of the most promising devices and represent the optimal technology to achieve 4D tracking [2]: they merge the fine segmentation of the silicon sensors [3, 4] with fast and enhanced signals to reach ~ 30 ps resolution for minimum ionizing particle (MIP) [5]. LGADs open the way for precise timing together with precise positioning. This can be explained by pointing out the key differences between a traditional sensor and an LGAD device, as shown in Figure 1. LGADs have an additional p-doping implant, the so-called Gain Layer (GL), surrounded by a Junction Termination Extension (JTE) structure. When depleted, the p-doping implant generates a high-electric-field region close to the detector surface: electrons drifting towards the cathode are accelerated by the high field and an avalanche due to impact ionization occurs. Exploiting the controlled charge multiplication in silicon, the LGAD design is such that yields low gain values and therefore low noise levels. Thanks to this, it is possible to improve the signal to noise ratio (SNR) limiting its drastic reduction with fluence, as it happens instead for standard silicon detectors. However, due to acceptor removal, the p^+ doping concentration of the gain layer gets reduced by irradiation and at a fluence of $1–2\times10^{15}$ n_{eq}/cm^2 the LGADs lose their multiplication power and behave as standard n-in-p sensors [2]. Acceptor removal is the transformation of electrically active dopant atoms into neutral defect complexes.

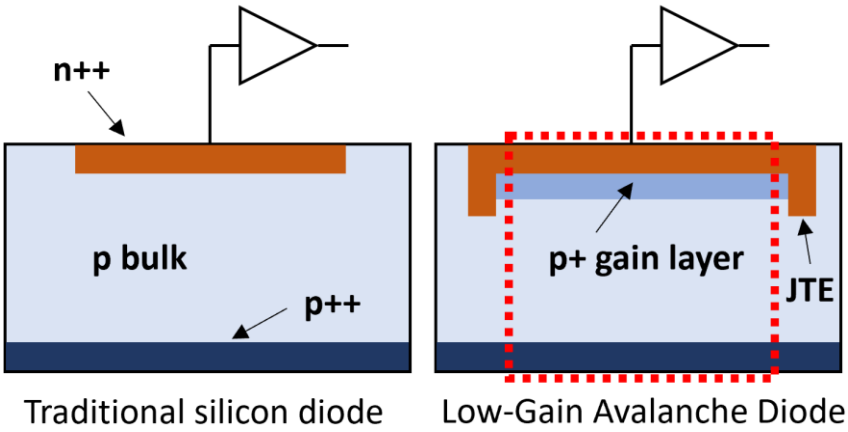

Fig. 1. Sketch of the differences between a traditional sensor (on the left) and a Low-Gain Avalanche Diode (on the right).

This work concerns the device-level simulations of non-irradiated and irradiated LGAD detectors with the aim to show how the developed radiation damage modeling

scheme can be used to predict the behavior of innovative heavily irradiated devices. Indeed, the developed model aims to predict the LGAD behavior up to the particle fluence operating conditions expected in the future collider experiments. To this purpose, state-of-the-art Synopsys Sentaurus TCAD suite of tools [6] has been adopted. The modeling scheme called "New University of Perugia" developed in the past [7, 8] has been fully implemented within the simulation environment to account for the effects of the radiation damage relying on a limited number of physics meaningful parameters. Moreover, the mechanism of acceptor removal in the multiplication layer has been considered by an analytical model coupled with the numerical model, in order to have a predictive insight into the electrical behavior and the charge collection properties of the LGAD detectors up to the highest particle fluences [9]. The comparison between simulated and measured I-V and C-V curves have been use as figure of merit for the model validation.

2. *TCAD simulation of LGAD devices*

2.1 Layout and doping profile

The layout of the simulated device has been designed in a quasi-mono dimensional domain, as can be seen in Figure 2. This helps to focus on its main performance because, neglecting the edge of the multiplication implant, the breakdown voltage is only due to the high electric field in the core region of the device (red dotted box in Figure 1). The highly doped n-type electrode and the moderately doped p-type region implanted below, where multiplication takes place, have been defined by Gaussian analytical profiles. The related peak doping concentration and the implantation depth have been carefully tuned since these parameters strongly influence the gain properties of the device. As represented in Figure 2, the peak dose of the multiplication layer has been properly reduced for increasing values of fluence, taking into consideration the acceptor removal mechanism for the irradiated structures. The p-type epitaxial layer has been described by a uniform doping concentration increasing with fluence, accounting of the acceptor creation, while an error function analytical profile has been considered for the backside highly doped p-type contact.

2.2 Physical and radiation damage models

The avalanche multiplication in silicon has been initially implemented by means of four different impact ionization models, which are the van Overstraeten-de Man [10], Okuto-Crowell [11], the University of Bologna [12] and Massey [13] ones. The Torino group provided us an external routine which computes the generation rate for Massey [14], because this model is not included in the commercial tool used for the TCAD simulations among the built-in functions.

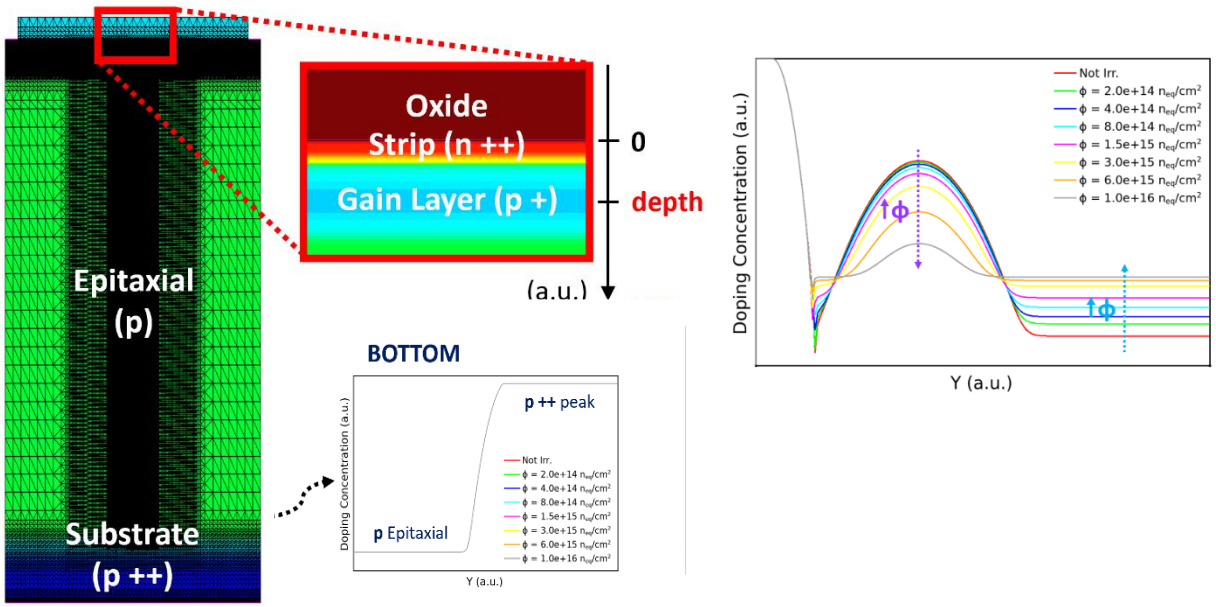

Fig. 2. Layout and doping profiles (Gaussian gain layer) of the simulated LGAD.

In order to model the comprehensive surface and bulk radiation damage effects in silicon by means of a limited set of physically meaningful deep-level radiation-induced traps, the radiation damage model "New University of Perugia" scheme [7-8, 15-17], has been used in the simulation framework. For what concern the acceptor removal mechanism in the multiplication layer, it has been implemented by the following analytical law:

$$N_{GL}(\phi) = N_A(0)e^{-c\phi}$$

according to that the peak dose of the gain layer profile N_{GL} is recomputed as a function of the fluence ϕ, the initial acceptor density $N_A(0)$ and a constant factor c which is calculated from the "Torino" parameterization [18]. Moreover, it has been determined experimentally that the acceptor creation can be described by the following analytical bulk parameterization, now called "Torino acceptor creation" parameterization:

$$N_{A,bulk} = \begin{cases} N_{A,bulk}(0) + g_c\phi & 0 < \phi \leq 3\text{E}15\,\text{n}_{\text{eq}}/\text{cm}^2 \\ 4.17\text{E}13 \cdot \ln(\phi) - 1.41\text{E}15 & \phi > 3\text{E}15\,\text{n}_{\text{eq}}/\text{cm}^2 \end{cases}$$

where g_c = 0.0237 cm^{-1} [19]. All results presented below are for a modified version of "Perugia 2019" where the doping concentration is a piecewise function. The model was named $PerugiaModDoping$. Initially, it was fine-tuned with data from PIN diodes and subsequently it was validated for LGADs. All magnitudes are presented in absolute

values.

2.3 Methodology developed

The adopted simulation flow follows the scheme described here. At first, the electrical characteristics of the device in terms of static and small-signal behavior have been simulated under different bias voltage and fluence conditions. The steady-state behavior of the irradiated device has been specifically simulated at 253 K, and then scaled to 300 K considering the temperature dependence of the bulk generation current [20], in order to compare the simulated data with the measurements. The active behavior of the device has been modelled by considering heavy ions impinging perpendicularly on the surface and traversing the whole device. In particular, the transient behavior has been carried out using a Minimum Ionizing Particle (MIP) equivalent stimulus taking into account the active thickness of the device [21].
By integrating the radiation-induced current signal in the time domain, the number of collected charges can be extracted. Performing the same procedure on a detector without any multiplication layer (i.e., a PIN diode), we defined the gain as the ratio between the collected charges in the LGAD over the ones of its corresponding reference diode. This implies that no contribution comes from the bulk, but only the multiplication layer is responsible of the device gain obtained. Such a gain definition is consistent with the experimental pursued procedure and therefore allows to have a direct comparison with the measurement data.

3. *Simulation results and comparison with measurements*

3.1 Effect of the avalanche model

Measurements concerning the static behavior of LGADs before irradiation have been compared to simulation findings. These have been carried out at room temperature comparing the four different impact ionization models mentioned before. The van Overstraeten-de Man, Okuto and University of Bologna models, due to the different value of the impact ionization coefficients used in these models, are not able to reproduce the experimental data, since they underestimate the breakdown voltage of the device. The dark black markers in Fig. 3 represent the experimental data, which are the result of an extensive campaign of measurements done by the Torino group on non-irradiated and irradiated LGAD devices [22]. The Massey model in Fig. 3 presents the best agreement with the experimental data, and for this reason all the simulations results shown in the next pages are based on the use of the Massey model for the avalanche mechanism.

3.2 Simulation outcomes and model validation

3.2.1 Steady-state and small-signal behavior

Figure 3 and 4 show the simulation results for the static and the small-signal behavior analyses. These have been carried out for a wide range of applied bias voltages, before and after irradiation. The I-V simulated curves represented with solid lines in Figure 3 point out the typical trend of the static behavior for increasing values of fluence, that is: the reduction of the “knee voltage” associated to the gain layer depletion, which is best

demonstrated by the C-V curves in Figure 4 (solid lines); the reduction of the I-V slope in the operating region of the sensor, until a constant plateau is reached for the highest values of fluence; the increase of both the breakdown voltage and the leakage current.

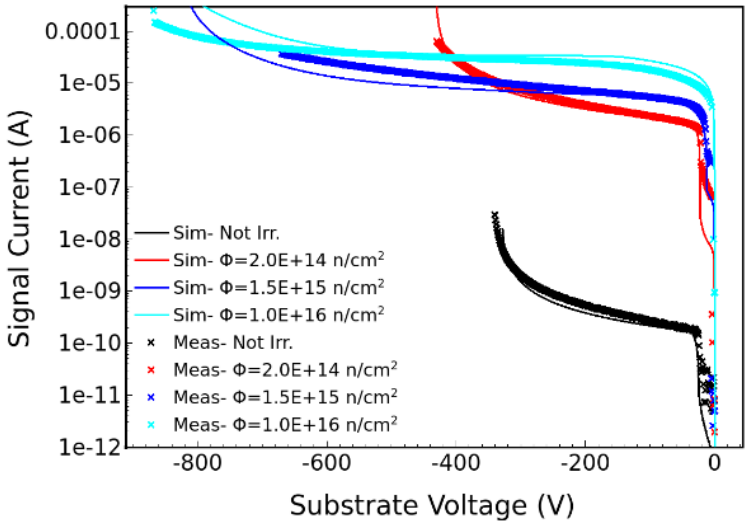

(a) (b)

Fig. 3. I-V simulated curves compared with experimental data before and after irradiation. Sensor area is 1 mm^2, thickness 55 µm and temperature 300 K.

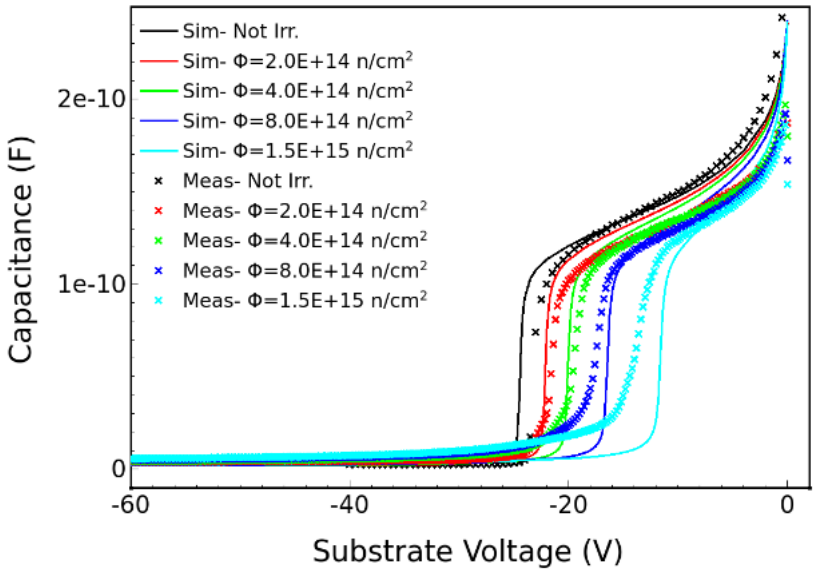

Fig. 4 C-V simulated curves compared with experimental data before and after irradiation. Sensor area is 1 mm^2, thickness 55 µm and temperature 300 K.

The simulated I-V and C-V curves are compared to the results obtained by measurements, before and after irradiation. The comparison for the non-irradiated devices shows a high accuracy of the data reproduction in simulation, starting from the gain layer depletion up to the device breakdown.

This good agreement has been also obtained for higher values of fluences, up to 1E16 n_{eq}/cm^2 in the case of the I-V characteristics.

3.2.2 Transient response and gain calculation

After the static and the small-signal analyses, the transient behavior of the LGAD device has been performed, considering the transient signals generated by the MIP stimulus both in the LGAD and in the reference diode. We have considered the device gain as the ratio of the charge collected by the LGAD to that collected by the reference diode. Therefore, we calculated the total charge of both devices by integrating the signal current over a period of 10 ns.

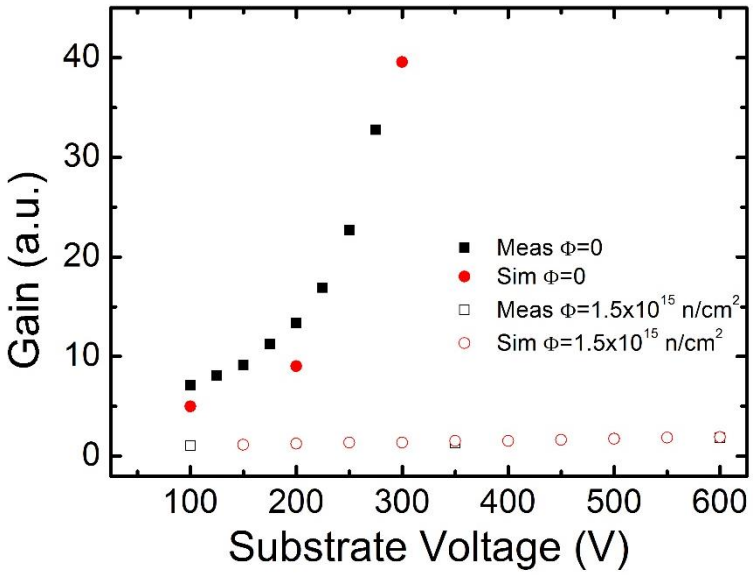

Fig. 5. Simulated gain compared to the measured one, before and after irradiation (fluence 1.5×10^{15} n_{eq}/cm^2).

In Figure 5 the calculated gain as a function of the bias voltage applied to the detector is reported and compared to experimental data, before and after irradiation. A very good agreement has been obtained for both non-irradiated and irradiated devices, as can be seen respectively in the curves of Figure 5. Indeed, the gain rises with the applied bias voltage, and as expected from measurements it undergoes a reduction for higher values of fluence, due to the acceptor removal mechanism.

The good agreement obtained between simulation results and experimental data has

allowed us to apply the newly developed model for the optimization of two innovative paradigms for the design of LGAD sensors for 4D tracking, namely i) compensated LGAD and ii) DC-Coupled Resistive Silicon Detectors (DC-RSD) LGADs. The first option refers to a new design of the gain layer implant that, by combining p^+ and n^+ dopants, has the potential to maintain a constant active doping density after very high irradiation. The second option is an evolution of RSD design that employs DC read-out with low resistivity strips between collecting pads.

4. Compensated LGAD

As described in the introduction, due to acceptor removal, the p^+ doping concentration of the gain layer gets reduced by irradiation. Dopant removal is the transformation of electrically active dopant atoms, both acceptors or donors, into neutral defect complexes. The removal by irradiation has been measured using different initial acceptor and donor densities, $N_{A,D}(0)$, and the effective doping concentration as a function of the fluence evolves as:

$$N_{A,D}(\phi) = N_{A,D}(0)e^{c_{A,D}\phi}$$

where c_A (c_D) is the acceptor (donor) removal rate which depends on the initial concentration. The higher the value of $N_{A,D}(0)$ and the lower is the value of $c_{A,D}$, hence the probability to experience dopant removal under irradiation. The addition of specific defects can mitigate the removal: oxygen and nitrogen co-implantation can reduce the donor removal [23], while the addition of carbon atoms prevents the acceptor removal [24]. Dopant removal can be further reduced by employing defect engineering.

A new paradigm for the gain layer design is necessary to overcome the present limit of radiation tolerance for the gain implant, to preserve internal signal multiplication up to the highest fluences. For this reason, we introduce an innovative design of the LGAD gain layer, the compensated gain layer. This breakthrough is described graphically in Fig. 6. As explained above, in a standard LGAD, due to the process of acceptor removal, the doping density of the gain implant (p-doped) decreases with irradiation, Fig. 6 (i) and (iii). In our design, which we call compensated LGAD, the effective doping of the gain implant is obtained by combining a p-doped and an n-doped implant. One possible outcome is shown in Fig. 6 (ii), where 2 parts of Phosphorus are used to balance 3 parts of Boron. If well-executed, in this design the n doping compensates part of the p doping, leaving effective doping similar to that used in the standard design. Both p and n implants will experience removal by irradiation, as it is shown in Fig. 6 (ii) and (iv).

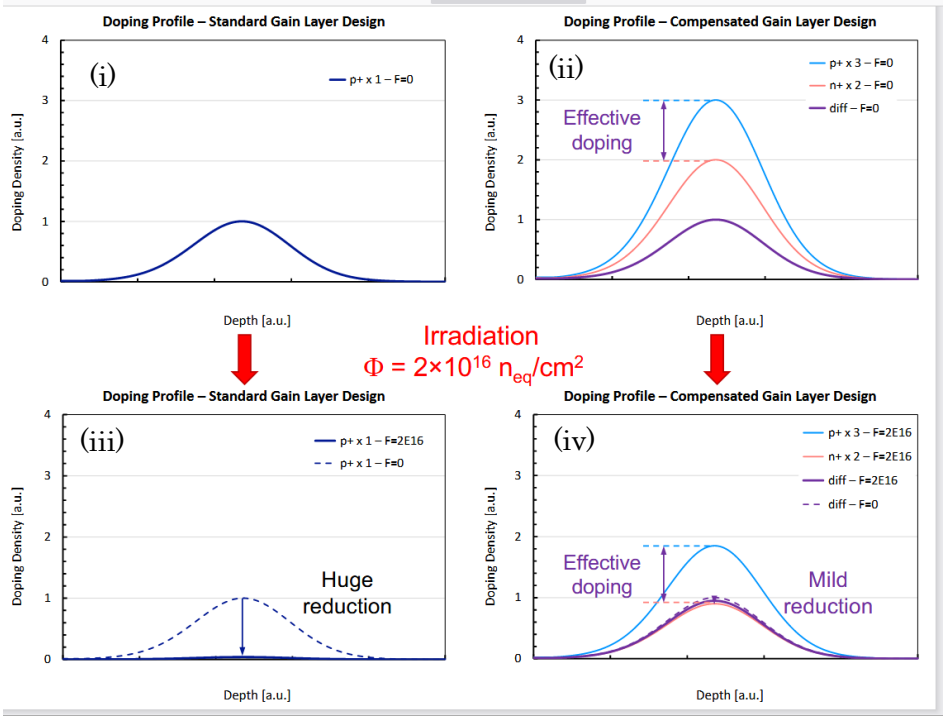

Fig. 6: Evolution with irradiation of the gain implant in (i, iii) and compensated (ii, iv) LGAD, after a fluence of 2×10^{16} n_{eq}/cm^2.

Under irradiation, three scenarios are possible:

1) The first one that where p and n removal coefficients are of the same order, and their difference will remain constant, yielding to an unchanged gain with irradiation. This is the best possible outcome.

2) The second option is when the p-atoms removal is faster than the n removal. This scenario is not as good as (1), but still leads to higher radiation resistance, as the overall rate of effective doping disappearance is slower than in the standard design. Moreover, co-implantation of carbon atoms can be used to mitigate the p-doping removal [18]. So, the addition of carbon can turn scenario (2) into (1).

3) The third option is when the n-atoms removal is faster, resulting in a rapid increase of the net p-doping. In this case, for equal bias voltage, the gain increases with irradiation. This situation can be handled by adding oxygen to the n implant, to decrease the n deactivation rate [23] or by a decrease of the bias voltage.

Taking into account that in literature n-atoms removal studies are limited to densities up to 1×10^{14} atoms/cm^3, it will be necessary to investigate the donor removal up to very high fluences using unexplored region of donor densities, between $\sim 1\times10^{16}$ and 1×10^{17} atoms/cm^3. Moreover, a dedicated study of the optimal parameters of oxygen co-implantation, such as density and temperature of activation, is needed to allow a level of understanding similar to the one achieved for carbon co- implantation.

Simulations of different production processes of compensated LGAD sensors has been performed using TCAD Silvaco [25], varying the Boron, chosen as p^+ dopant, and Phosphorus, chosen as the n^+ counterpart. Three different conditions have been considered: in the first one 4 parts of Phosphorus are used to balance 5 parts of Boron, in the second 2 parts of Phosphorus are used to balance 3 parts of Boron and in the last 1 part of Phosphorus is used to balance 2 parts of Boron. There are no differences in the electrical behavior in these three cases, for not irradiated devices.

Considering the last condition, we have deeply investigated the properties of the compensated gain layer by analyzing three different shapes of the implant profiles together with two different diffusion mechanisms: high (case bb) and low (case aa). The boron diffusion reveals to be crucial for a suitable gain layer design and by exploiting the potentiality of the TCAD simulation approach it is possible to obtain a predictive insight of the electrical behavior of devices before the actual manufacturing process. The steady-state behavior of the compensated LGAD sensors has been simulated using TCAD, to investigate the overall performances of the new design and how the doping transition regions observed in the gain layer volume can affect the sensors' operation. Fig. 7 shows the dark current evolution as a function of the reverse bias for the six combinations of implant profiles and diffusion considering a PIN diode as reference.

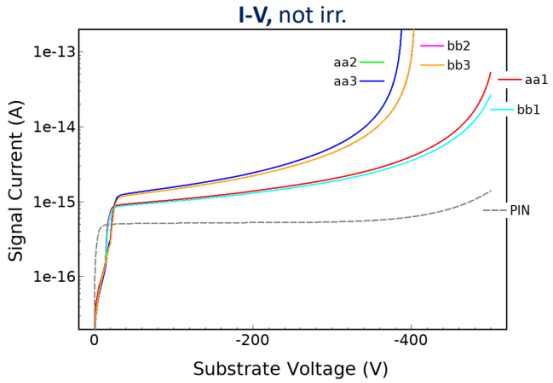

Fig. 7 Simulated current–voltage characteristics for compensated LGAD sensors with three different combinations of implant profile shapes (1, 2, 3) and two different diffusion mechanisms (aa-low and bb-high), for not irradiated devices. The current–voltage characteristic of a standard PIN sensor is included for reference.

5. A new design of resistive silicon detector: DC-RSD

Resistive Silicon Detector (RSD) is an LGAD optimized for both spatial and timing (4D-tracking), which make use of an AC-coupled read-out electronics and a continuous gain implant without any segmentation. It combines the excellent timing capabilities of LGAD with remarkable space resolution, making it one of the emerging technologies for 4D tracking. The major peculiarity of the RSD paradigm is the use of a continuous

n^+-resistive electrode and a continuous p^+-gain layer, allowing 100% of fill factor, respect the standard LGAD affected by the lack of gain in the inter-pad region. On the other hand, different drawbacks are linked to the nature of RSD paradigm, e.g. the bipolar behavior of the signals due to the use of the AC-coupled read-out, the baseline fluctuation due to the collection of the leakage current at the edge of the sensor, and the position-dependent resolution [26-28]. The DC-coupled RSD – or DC-RSD, enables to cope with these issues, by eliminating the dielectric and using a DC-coupling to the electronics, while maintaining the advantage of 100% fill factor.

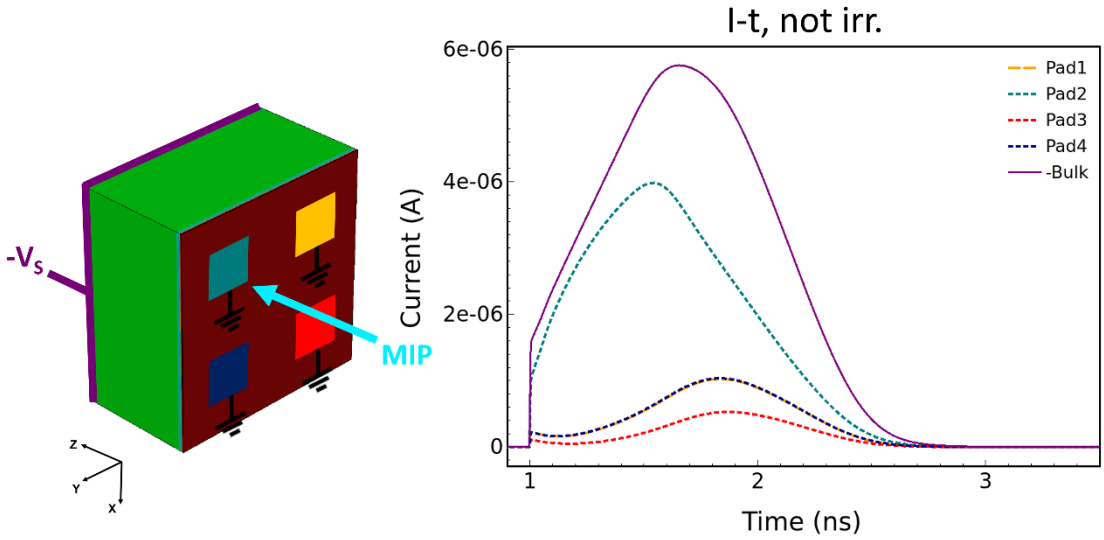

Fig. 8. TCAD simulated signals (right) generated by a MIP heavy ion in a 50 µm-pitch four-pad DC-RSD detector (left), biased at 200 V, at room temperature. Gray, yellow, red and blue navy lines represent the signals coming from the pads, while the violet line represents the signal read from the contact on the back.

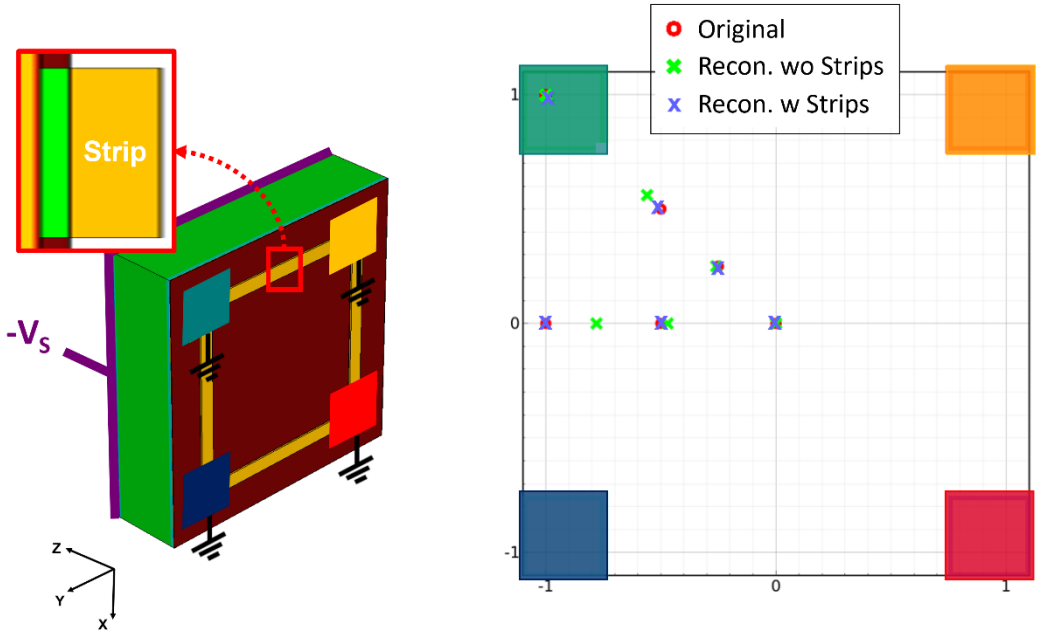

Fig. 9. Map of the reconstructed particle impinging positions obtained by the combination of the charge extracted from the signals read by the four pads, showing a better accuracy of the position reconstruction in the case of DC-RSD flavor characterized by the strip-connected pads (blue markers).

Several challenges are related to the simulation of DC-RSD, due to the nature of its design and the large pixel size of the order of a few millimeters. Full-3D TCAD simulation have been carried out in order to analyze the device behavior in terms electrical properties and response after the passage of a charged particle. In Fig. 8, the transient behavior is described by the current-time curves. The response of the device after the passage of a charged particle (e.g., a minimum ionizing particle - MIP), is represented by the gray, yellow, red and blue navy curves, which are the currents read out by the four pads, and by the violet curve, which is the current read out on the back contact. As already shown by the Spice simulations [29], the higher the sheet resistance, the lower and wider the read-out signals, worsening the timing capabilities of the detector. The position reconstruction methodology has been described in a previous work [29] and straightforwardly implemented within the TCAD environment. Moreover, by simulating the passage of a charged particle, e.g. a MIP, it has been proved that the distortion is strongly reduced if the read-out electrodes are connected with low-resistivity strips (see Figure 9 right). The accuracy of the position reconstruction improves when inter-pad resistive strips are used, because they help to confine the signal spreading within the pixel. A new batch of TCAD simulations, taking into account the radiation damage effects, is in progress. Such results will provide all the necessary information for the first batch of DC-RSD produced by Fondazione Bruno Kessler (FBK) foundry in Trento, Italy.

6. Conclusions

This paper presents a strategy for the numerical simulation of LGAD devices before and after irradiation. All the simulation results well reproduce the experimental data, thus

demonstrating the reliability of the implemented simulation framework. Aiming at considering the radiation damage effects, a combination of the "New University of Perugia TCAD model" and the acceptor removal one has been used. Thanks to this, it has been possible to reproduce experimental data with high accuracy, demonstrating the reliability of the implemented simulation framework. Moreover, the good agreement obtained between simulation results and experimental data has allowed us to apply the newly developed model for the optimization of two innovative paradigms for the design of LGAD sensors for 4D tracking, namely i) compensated LGAD and ii) DC-Coupled Resistive Silicon Detectors (DC-RSD) LGADs. TCAD simulations with the validated model support the ongoing activities, oriented both to the comparison with the experimental data and to the design of the future productions of innovative LGADs.

Acknowledgments

The authors acknowledge funding from the European Union's Horizon 2020 research and innovation program under GA No 101004761 and from the Italian PRIN MIUR 2017 (Research Project "4DInSiDe" – Innovative Silicon Detectors for particle tracking in 4Dimensions). This work is held in collaboration with the INFN CSN5 "eXFlu" research project.

References

[1] H. Sadrozinsky et al., Rep. Prog. Phys., vol. 81, no. 2 (2018).
[2] N. Cartiglia et al., Nucl. Instrum. Meth. A 924, 350 (2019), doi:10.1016/j.nima.2018.09.157
[3] G. Paternoster et al., Nucl. Instrum. Meth. A 987 (2021) 164840, Ministero dell'Università e della Ricerca, MUR - BANDO 2022. doi: 10.1016/j.nima.2020.164840
[4] M. Tornago et al., Nucl. Instrum. Meth. A 1003 (2021) 165319, doi: 10.1016/j.nima.2021.165319
[5] N. Cartiglia et al., Nucl. Instrum. Meth. A 850, (2017) 83, doi: 10.1016/j.nima.2017.01.021
[6] Synopsys Sentaurus Device User Guide, S-2021.06-SP1 .
[7] A. Morozzi et al., Front. Phys., February 2, (2021), DOI: 10.3389/fphy.2021.617322.
[8] Asenov, P., Arcidiacono, R., Cartiglia, N., et al, Nuclear Inst. and Methods in Physics Research, A 1040, 167180 (2022).
[9] G. Kramberger et al., JINST **10** P07006 (2015), DOI: 10.1088/1748-0221/10/07/P07006.
[10] R. van Overstraeten et al., Solid-State Electronics, vol. 13, no. 1, pp. 583-608 (1970).
[11] Y. Okuto et al., Threshold Energy Effect on Avalanche Breakdown Voltage in Semiconductor Junctions, Solid-State Electronics, vol. 18, no. 2, pp. 161-168 (1975).
[12] M. Valdinoci et al., International Conference on Simulation of Semiconductor Processes and Devices (SISPAD), Kyoto, Japan, pp. 27-30 (1999).
[13] D. J. Massey, et al., IEEE Transactions on Electron Devices, vol. 53, no. 9, pp. 2328-2334 (2006).
[14] M. Mandurrino et al., IEEE Nuclear Science Symposium and Medical Imaging Conference (NSS/MIC), October 21-28 (2017), DOI: 10.1109/NSSMIC.2017.8532702.
[15] A. Morozzi et al., JINST 11 C12028 (2016).
[16] F. Moscatelli et al., JINST 12 P12010 (2017).
[17] F. Moscatelli; D. Passeri; A. Morozzi; S. Mattiazzo; G. -F. Dalla Betta; M. Dragicevic; G. M. Bilei, IEEE Transactions on Nuclear Science, Volume: 64, 8 (2017).
[18] M. Ferrero et al., Nucl. Inst. And Meth. in Phys. Res. A, November 30 (2018), DOI: 10.1016/j.nima.2018.11.121.
[19] M. Ferrero, et al., (2019), Online https://indico.cern.ch/event/812761/contributions/3459068/.
[20] A. Chilingarov, JINST **8** P10003 (2013).
[21] S. Meroli et al., JINST **6** P06013 (2011).

[22] V. Sola et al., Nucl. Inst. And Meth. in Phys. Res. A, July 21 (2018), DOI: 10.1016/j.nima.2018.07.060.
[23] M. Moll et al., Nucl. Instrum. Meth. A 439 282 (2000), doi: 10.1016/S0168-9002(99)00842-6
[24] I. Mandic et al., J. Instrum. 15 P11018 (2020), doi:10.1088/1748-0221/15/11/P11018.
[25] SILVACO, Semiconductor Process and Device Simulation, URL: https://silvaco.com/tcad.
[26] M. Tornago et al., Nucl. Instrum. Meth. A 1003, 165319 (2021).
[27] M. Mandurrino et al., IEEE Electron Device Letters, vol. 40, no. 11, pp. 1780-1783(2019).
[28] G. Giacomini et al., Fabrication and performance of AC-coupled LGADs, JINST 14 P09004 (2019).
[29] L. Menzio et al. Nuclear Inst. and Methods in Physics Research, A 1041, 167374 (2022).